Fabrication and characterization of topological insulator Bi_2Se_3 nanocrystals

S. Y. F. Zhao,[1] C. Beekman,[1] L. J. Sandilands,[1] J. E. J. Bashucky,[1] D. Kwok,[2] N. Lee,[2] A. D. LaForge,[3] S. W. Cheong,[2] and K. S. Burch[1,a)]
[1]*Department of Physics and Institute of Optical Sciences, University of Toronto, 60 St. George Street, Toronto ON M5S 1A7, USA*
[2]*Department of Physics and Astronomy, Rutgers Center for Emergent Materials, Rutgers University, 136 Frelinghuysen Road, Piscataway, New Jersey 08854, USA*
[3]*Department of Physics, University of California, Santa Cruz, 1156 High Street, Santa Cruz, California 95064, USA*

(Received 14 December 2010; accepted 3 March 2011; published online 6 April 2011)

In the recently discovered class of materials known as topological insulators, the presence of strong spin-orbit coupling causes certain topological invariants in the bulk to differ from their values in vacuum. The sudden change in invariants at the interface results in metallic, time reversal invariant surface states whose properties are useful for applications in spintronics and quantum computation. However, a key challenge is to fabricate these materials on the nanoscale appropriate for devices and probing the surface. To this end we have produced 2 nm thick nanocrystals of the topological insulator Bi_2Se_3 via mechanical exfoliation. For crystals thinner than 10 nm we observe the emergence of an additional mode in the Raman spectrum. The emergent mode intensity together with the other results presented here provide a recipe for production and thickness characterization of Bi_2Se_3 nanocrystals. © *2011 American Institute of Physics*. [doi:10.1063/1.3573868]

Topological metallic surface states are predicted to have numerous properties that are useful for spintronics and quantum computation.[1,2] A challenging aspect of this research has been to isolate surface state contributions to the measured properties of topological insulators.[3–7] Studying nanometer thick crystals allows one to tune the chemical potential with electric field,[8–12] as well as observe modifications of the excitation spectrum produced by interactions of top and bottom surfaces.[11,13–16] One option for producing thin crystals is mechanical exfoliation. This method, together with Raman spectroscopy, has proven to be extremely fruitful in the study of graphene[17,18] and other nanocrystals.[19,20] Indeed, Raman provides direct access to the phonon spectrum and can be used to map the thickness[17,21] or doping level[22] over a large area.

Similar studies of the topological insulators Bi_2Se_3 and Bi_2Te_3 have been attempted. To date, these experiments have been limited to exfoliated Bi_2Se_3 crystals >10 nm thick[12,23,24] or Bi_2Te_3 where the bulk gap is small.[8,9] A limiting factor in these experiments was the strong optical absorption of these compounds, making the identification of thin crystals difficult on Si/SiO_2 substrates. With this in mind, we have mechanically exfoliated Bi_2Se_3 crystals on Mica, enabling us to optically identify crystals only 2 nm thick. By systematically studying these crystals with Raman spectroscopy and optical and atomic force microscopies (AFM) we have devised a method for characterizing the thickness of Bi_2Se_3 nanocrystals using noninvasive, all-optical methods. Specifically, an additional mode appears in the Raman spectra for ultrathin (<10 nm) crystals. The observed thickness dependence of the emergent mode intensity can be used for thickness verification of nanocrystals via Raman measurements.

Bi_2Se_3 forms a rhombohedral lattice in which the unit cell is composed of three five-layer stacks known as quintuple layers (QLs). A unit cell measures 2.87 nm along the c axis, and 1 QL is $\approx$0.96 nm thick.[25] Atoms are arranged into planar hexagonal sheets with the sequence $-[Se^{(2)}-Bi-Se^{(1)}-Bi-Se^{(2)}]-$.[26] The superscripts indicate the structural in-equivalence of the Se ions, with the $Se^{(1)}$ atom at a center of inversion within a QL. Therefore, one expects phonon modes to be exclusively infrared (IR) or Raman active. The weak van der Waals bonds between neighboring $Se^{(2)}$ planes enables mechanical exfoliation. Ultrathin Bi_2Se_3 nanocrystals could be identified after exfoliation by optical microscopy in transmission mode. The crystal thickness was subsequently determined using AFM.[26]

Raman spectroscopy (λ=532 nm, spot size $\sim$1 μm) confirmed that these nanocrystals are indeed Bi_2Se_3 and was used to study the evolution of the crystal lattice structure with thickness. A raman spectrum ($I(\omega)$) for a bulk crystal is shown in Fig. 1(a), where we observe a strong phonon mode at 175 cm^{-1} and the onset of a mode below 150 cm^{-1}. Previous results[25] suggest the higher energy mode corresponds to a Raman active A_{1g} mode and the latter to an E_g mode, in accord with group theory predictions for phonons at the Brillouin zone center (q=0) probed by optical experiments. Indeed, the five atoms in the unit cell should lead to 12 optical modes, each of which is either exclusively Raman or IR active.[25] We also observe a broad shoulder between 200 and 350 cm^{-1}, similar to a feature observed in a recent IR study of bulk Bi_2Se_3 [see Fig. 2(b)].[27] The presence of this feature in both Raman as well as IR and its broad lineshape suggest that it is due to two-phonon excitations.

To quantitatively analyze the evolution of the spectra, we fit the measured Raman data with multiple Lorentzian oscillators in the form: $I(\omega)=I_0+\Sigma_i(A_i\Gamma_i/(4(\omega-E_i)^2+\Gamma_i^2))$ where i ranges from 1 to 3 or 4, depending on thickness, I_0 accounts for the background, E_i is the center, Γ_i is the width, and A_i is the area of peak i. The resulting fit for the bulk spectrum

a)Electronic mail: kburch@physics.utoronto.ca.

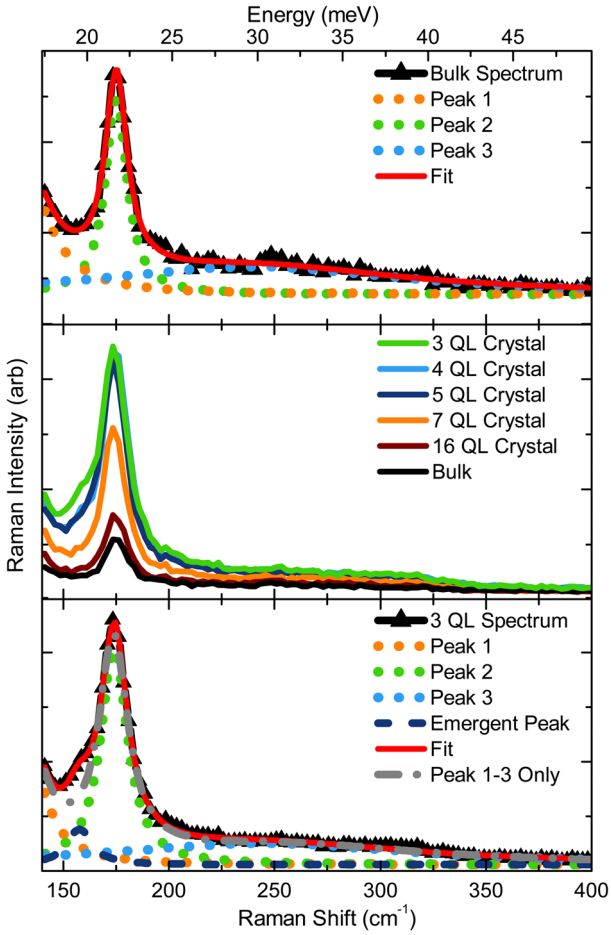

FIG. 1. (Color online) Raman spectra for Bi_2Se_3. (a) Spectrum for the bulk crystal (line+symbols) with the corresponding fit (solid line) consisting of three Lorentzian oscillators (dotted lines). (b) Spectra for crystals of varying thicknesses, 3→16 QL and bulk. (c) Spectrum for 3QL nanocrystal. The data (line+symbols) is fit with four Lorentzian oscillators (solid line). The fit resulting from three oscillators is shown for comparison (dashed dotted line).

with three oscillators is shown in Fig. 1(a), where the center frequency of the E_g mode (peak 1) was fixed at 131.5 cm^{-1} based on previous studies.[25] Turning to Fig. 1(b) we examine the evolution of the Raman spectra with varying crystal thicknesses, where an enhancement of the overall signal is observed with decreasing number of QL. As is discussed

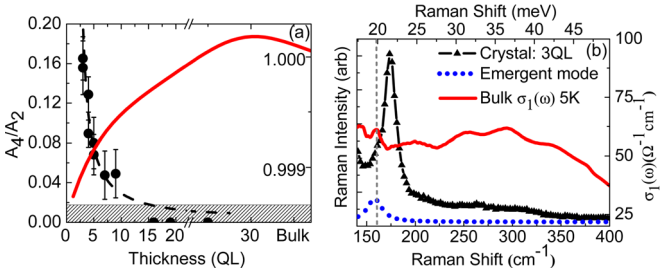

FIG. 2. (Color online) (a) Ratio of emergent peak intensity to the main peak intensity (determined from fits) as function of crystal thickness. The dashed line is a guide to the eye and plotted to show the $(\alpha/(QL-2))$ trend of the ratio. The gray area for $A_4/A_2<0.02$ indicates the detection limit of our system. The ratio A_4/A_2 as function of crystal thickness due to FP effects (solid line, right axis). (b) Left axis: Raman spectrum for a 3 QL thick crystal (line+symbols) and the Lorentzian corresponding to the emergent mode (dotted line). Right axis: optical conductivity data (solid line) of a bulk Bi_2Se_3 single crystal taken at T=5 K.

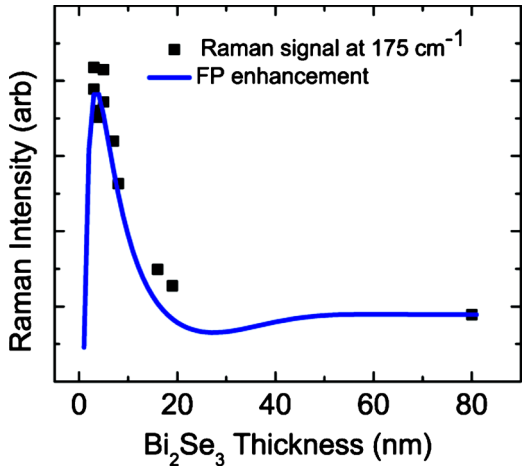

FIG. 3. (Color online) Raman intensities as function of crystal thickness at 175 cm^{-1} (squares) and calculated Raman intensities due to FP interference effects (solid line: optical constants modified from bulk values).

below this enhancement results from multiple reflections in the Bi_2Se_3 crystal. Perhaps more surprisingly, an additional mode emerges at 158 cm^{-1} as the crystal thickness is reduced [see Fig. 1(c)]. Indeed, the use of only three oscillators, which worked well for crystals thicker than 10 QL [Fig. 1(a)], results in a large difference around 158 cm^{-1} between the fit (dashed dotted line) and the spectrum. By simply adding another mode ($i=4$), the fit (solid line) agrees very well with the data. The emergence of the mode at 158 cm^{-1} for ultrathin crystals suggests it can be used to verify sample thickness.

We explore this possibility in Fig. 2, where we plot the ratio of the emergent mode intensity with the main peak intensity (A_4/A_2). For thicknesses below 10 QL this ratio increases and agrees well with $\alpha/(QL-2)$ behavior (dashed line), which corresponds to the relative weight of surface and bulk modes. Indeed, the intensity of a particular mode is proportional to the volume over which the light can emanate. For a surface mode, this volume is independent of thickness. In contrast, for a bulk mode the volume probed is proportional to the crystal thickness (for thicknesses less than the penetration depth). Unfortunately, due to the detection limit of our instrument, we are not able to convincingly detect the mode for $A_4/A_2<0.02$.

While the mode appears to have its origin in the surface, it could also be due to Fabry–Perot (FP) interference in the Mica substrate. To rule this out, we repeatedly performed Raman spectroscopy on a single 3 QL nanocrystal and subsequently cleaved the back surface of the Mica to reduce its thickness. The resultant spectra all overlapped (not shown), implying that FP interference in the Mica substrate can be neglected. Nonetheless, for a fixed substrate thickness, the interference effects due to multiple reflections in the Bi_2Se_3 nanocrystals will change as the crystals are thinned. To check the FP effects on the Raman spectra we have performed a calculation similar to the one shown to work well in graphene and $Bi_2Sr_2CaCu_2O_8$ nanocrystals.[20,21] In Fig. 3, we plot the measured and the calculated intensity (FP model) as a function of crystal thickness for the main mode (175 cm^{-1}). Changes in the ratio (A_4/A_2) due to FP effects are plotted in Fig. 2(a) and only reveals a very small dependency on crystal thickness, which is opposite to what we

observe. Therefore, the emergent mode is intrinsic to Bi_2Se_3 nanocrystals and not caused by FP effects. However, Fig. 3 shows that the change in the overall Raman signal with crystal thickness is explained by FP interference effects only if the optical constants are modified from the bulk values. This modification is not unreasonable given recent photoemission experiments.[14,16] Interestingly, these data also show the utility of Raman measurements, as the overall intensity can be used to determine the thickness of the Bi_2Se_3 nanocrystals.

While the FP interference described above can account for the overall intensity- thickness trends in Fig. 1, the origin of the 158 cm^{-1} mode remains unclear. Interestingly, an additional mode also appeared in Raman spectra of nanocrystals of the isostructural topological insulator Bi_2Te_3.[8] This mode matched perfectly the frequency of an IR-active mode and so it was attributed to the breaking of inversion symmetry. Shahil *et al.* suggested that mechanical exfoliation resulted in breaks within a QL as well as between them. A similar explanation may be appropriate for Bi_2Se_3: a recent IR reflectance study of the bulk revealed a mode with the same frequency and width[27] [see Fig. 2(b)]. However, in Bi_2Te_3 this mode appeared in crystals thinner than 84 nm, whereas it only appears in Bi_2Se_3 nanocrystals thinner than 10 nm. We believe the mode may be due to the built-in electric fields at the surface. Specifically, the band bending inherent to materials with surface states will generate an electric field that will break the inversion symmetry.

We have shown that Raman spectroscopy is an effective nanometrology tool for identifying nanocrystals of the topological insulator Bi_2Se_3. This is accomplished by monitoring (i) the overall intensity of the Raman signal and/or (ii) the strength of the emergent mode at 158 cm^{-1}. The overall thickness dependence of the intensity can be accounted for by proper modeling of the effect of interference on the Raman spectra. The origin of the emergent mode remains unclear, although the presented optical conductivity data suggests that inversion symmetry breaking leads to an IR mode becoming Raman active. However, it is interesting to note that the emergent mode appears for the same thickness regime of Bi_2Se_3 for which a gap has been theorized to open due to coupling of the two surfaces.[14,16] In addition, the polar surface of Mica may lead to band bending, which breaks inversion symmetry. Therefore performing Raman spectroscopy on a suspended crystal would provide conclusive determination of the influence of the Mica substrate on the Bi_2Se_3 nanocrystals. Nonetheless, we have provided a path for fabricating and identifying Bi_2Se_3 nanocrystals through the combination of mechanical exfoliation on transparent substrates and the use of Raman spectroscopy. This work paves the way for future devices and studies of the surface states of topological insulators.

We are grateful for numerous discussions with Y. B. Kim and H. Y. Kee and we thank Y. J. Choi for the transport measurement. Work at the University of Toronto was supported by NSERC, CFI, and ORF; work at Rutgers University was supported by the NSF under Grant No. NSF-DMR-0804109.

[1] J. Moore, Nat. Phys. **5**, 378 (2009).
[2] H. Zhang, C. Liu, X. Qi, X. Dai, Z. Fang, and S. Zhang, Nat. Phys. **5**, 438 (2009), and references therein.
[3] H. Peng, K. Lai, D. Kong, S. Meister, Y. Chen, X.-L. Qi, S.-C. Zhang, Z.-X. Shen, and Y. Cui, Nature Mater. **9**, 225 (2010).
[4] K. Eto, Z. Ren, A. A. Taskin, K. Segawa, and Y. Ando, Phys. Rev. B **81**, 195309 (2010).
[5] J. G. Analytis, J.-H. Chu, Y. Chen, F. Corredor, R. D. McDonald, Z. X. Shen, and I. R. Fisher, Phys. Rev. B **81**, 205407 (2010).
[6] T. Zhang, P. Cheng, X. Chen, J.-F. Jia, X. Ma, K. He, L. Wang, H. Zhang, X. Dai, Z. Fang, X. Xie, and Q.-K. Xue, Phys. Rev. Lett. **103**, 266803 (2009).
[7] S. R. Park, W. S. Jung, C. Kim, D. J. Song, C. Kim, S. Kimura, K. D. Lee, and N. Hur, Phys. Rev. B **81**, 041405 (2010).
[8] K. M. F. Shahil, M. Z. Hossain, D. Teweldebrhan, and A. A. Balandin, Appl. Phys. Lett. **96**, 153103 (2010).
[9] D. Teweldebrhan, V. Goyal, and A. A. Balandin, Nano Lett. **10**, 1209 (2010).
[10] Z. Ding, S. K. Bux, D. J. King, F. L. Chang, T.-H. Chen, S.-C. Huang, and R. B. Kaner, J. Mater. Chem. **19**, 2588 (2009).
[11] Y. Sakamoto, T. Hirahara, H. Miyazaki, S.-i. Kimura, and S. Hasegawa, Phys. Rev. B **81**, 165432 (2010), and references therein.
[12] J. G. Checkelsky, Y. S. Hor, R. J. Cava, and N. P. Ong, arXiv:1003.3883v1 (unpublished).
[13] J. Linder, T. Yokoyama, and A. Sudbø, Phys. Rev. B **80**, 205401 (2009).
[14] C.-X. Liu, H. Zhang, B. Yan, X.-L. Qi, T. Frauenheim, X. Dai, Z. Fang, and S.-C. Zhang, Phys. Rev. B **81**, 041307 (2010).
[15] H.-Z. Lu, W.-Y. Shan, W. Yao, Q. Niu, and S.-Q. Shen, Phys. Rev. B **81**, 115407 (2010).
[16] Y. Zhang, K. He, C.-Z. Chang, C.-L. Song, L.-L. Wang, X. Chen, J.-F. Jia, Z. Fang, X. Dai, Y.-W. Shan, S.-Q. Shen, Q. Niu, X.-L. Qi, S.-C. Zhang, X.-C. Ma, and Q.-K. Xue, Nat. Phys. **6**, 584 (2010).
[17] A. Gupta, G. Chen, P. Joshi, S. Tadigadapa, and P. C. Eklund, Nano Lett. **6**, 2667 (2006).
[18] A. B. Kuzmenko, L. Benfatto, E. Cappelluti, I. Crassee, D. van der Marel, P. Blake, K. S. Novoselov, and A. K. Geim, Phys. Rev. Lett. **103**, 116804 (2009), and references therein.
[19] L. M. Malard, M. A. Pimenta, G. Dresselhaus, and M. S. Dresselhaus, Phys. Rep. **473**, 51 (2009).
[20] L. J. Sandilands, J. X. Shen, G. M. C. F. Zhao, S. Ono, Y. Ando, and K. S. Burch, Phys. Rev. B **82**, 064503 (2010).
[21] D. Yoon, H. Moon, Y.-W. Son, J. S. Choi, B. H. Park, Y. H. Cha, Y. D. Kim, and H. Cheong, Phys. Rev. B **80**, 125422 (2009).
[22] D. M. Basko, S. Piscanec, and A. C. Ferrari, Phys. Rev. B **80**, 165413 (2009), and references therein.
[23] H. Steinberg, D. R. Gardner, Y. S. Lee, and P. Jarillo-Herrero, arXiv:1003.3137 (unpublished).
[24] B. Sacepe, J. B. Oostinga, J. Li, A. Ubaldini, N. J. G. Couto, E. Giannini, and A. F. Morpurgo, arXiv:1101.2352v1 (unpublished).
[25] W. Richter and C. R. Becker, Phys. Status Solidi B **84**, 619 (1977).
[26] See supplementary material at http://dx.doi.org/10.1063/1.3573868 for the crystal structure of Bi_2Se_3 and an AFM image and the thickness determination.
[27] A. D. LaForge, A. Frenzel, B. C. Pursley, T. Lin, X. Liu, J. Shi, and D. N. Basov, Phys. Rev. B **81**, 125120 (2010).

Supplemental material corresponding to manuscript: Fabrication and Characterization of Topological Insulator Bi_2Se_3 Nanocrystals

S.Y.F. Zhao[1], C. Beekman[1], L.J. Sandilands[1], J.E.J. Bashucky[1], D. Kwok[2], N. Lee[2], A.D. LaForge[3], S.W. Cheong[2] and K.S. Burch[1a)]

[1]*Department of Physics & Institute of Optical Sciences, University of Toronto, 60 St. George Street, Toronto, ON M5S 1A7*

[2]*Rutgers Center for Emergent Materials and Department of Physics and Astronomy, Rutgers University, 136 Frelinghuysen Road, Piscataway, NJ 08854, USA.*

[3]*Department of Physics, University of California, Santa Cruz, 1156 High Street, Santa Cruz, California 95064, USA.*

Exfoliation. Bulk Bi_2Se_3 crystals with structure shown in Fig. S1 were prepared as described elsewhere[1]. The crystals were then mechanically exfoliated onto a Mica substrate (Structure Probe Inc, muscovite V1), in a manner similar to the preparation of graphene an B2212[2]. Mica was chosen for exfoliation since it is optically transparent and provides atomically flat, polar surfaces. This leads to an enhanced yield and eases the identification of nanocrystals. However, to maintain the pristine surface of the Mica, exfoliation was performed in a sealed box under an Argon atmosphere. This maximized yield of thin crystals and minimized the adhesion of contaminants on the substrate surface. To further minimize water adhesion, substrates were heated to 150°C before exfoliation, and Bi_2Se_3 was deposited onto a freshly cleaved layer of Mica.

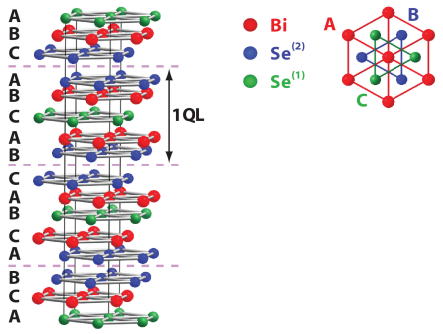

FIG. S1. Crystal structure of Bi_2Se_3. A QL consists of a stack of five planes $Se^{(2)}$-Bi-$Se^{(1)}$-Bi-$Se^{(2)}$. Within the planes atoms have a triangular lattice (HCP) with three possible positions of the plane (A, B and C). The QLs are separated by van der Waals bonds (dashed lines) between $Se^{(2)}$-$Se^{(2)}$ planes.

Optical and Atomic Force Microscopy. A typical optical microscope image is shown in Fig. S2a, which demonstrates the high yield of crystals that is achieved with our exfoliation method. More importantly, ultrathin crystals with a thickness of only a few QLs, were found regularly and crystals down to approximately 2 QL showed optical contrast in transmission. The thickness of the nanocrystals was subsequently measured via contact mode atomic force microscopy (AFM), an example image is shown in Fig. S2b. In Fig. S2c a profile measured along the line indicated in Fig. S2b is shown, clearly indicating the structural integrity of the nanocrystals. In addition we have performed scanning electron microscopy (SEM) and energy dispersive X-ray spectroscopy (EDX) to confirm the integrity of our nanocrystals.

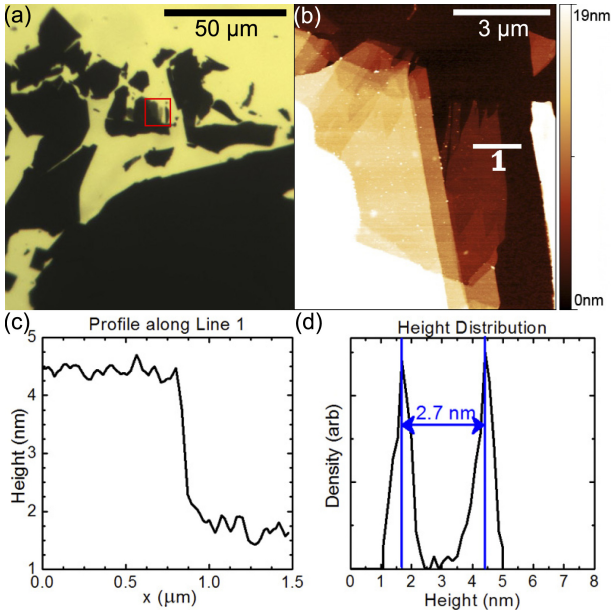

FIG. S2. (a) Optical microscope image of nanocrystals in transmission mode, the scale bar is 50 μm. Black regions correspond to thick crystals, with thinner nanocrystals appearing grey. The red box indicates the region imaged by AFM. (b) AFM image of the 3QL crystal with the corresponding color bar and the scale bar is 3 μm. (c) Profile across the 3QL crystal, cut along the line shown in B. (d). Histogram of the height distribution around the edge of the 3QL crystal (shown in B). Crystal thickness is determined from the separation between the observed peaks, which in this case is 2.7 nm.

The nanocrystal thickness was determined through AFM by taking a histogram of the height distribution around the edge of the crystal (Fig. S2d). Such histograms show two peaks and crystal thickness is determined from the distance between the observed peaks. For the crystal shown in Fig. S2b this is 2.7 nm (3QL).

Raman Spectroscopy. The Raman spectra were taken in a backscattering configuration with a Horiba Jobin Yvon LabRam microscope with a 532 nm excitation source and a 100x objective (0.8 NA) resulting in an $\approx$ 1 μm spot size.

a)Electronic mail: kburch@physics.utoronto.ca

In accord with previous experiments on exfoliated Bi_2Te_3[3,4], we found Bi_2Se_3 nanocrystals burn easily with laser exposure, and a careful study of laser powers and exposure times to minimize damage and maximize signal to noise ratios was performed. Highly reproducible spectra result from a power of 15 μW with exposure times of 2 minutes and an equivalent time without exposure, to allow the sample to cool.

Scanning Electron Microscopy (SEM) and Energy Dispersive X-ray Spectroscopy (EDX) In addition we also present the SEM and EDX characterization of the Bi_2Se_3 nanocrystals. The SEM images (Figs. S3a and B, V_{acl} = 2 kV and I_{beam} = 20 μA) show the high yield and integrity of the crystals. The integrity is confirmed by the EDX characterization (Fig. S3c, black line) which shows that the crystals contain both Bi and Se with their ratio equal to 0.3. Since we performed standardless EDX it is not possible to accurately determine stoichiometry from the spectrum. However, comparing this spectrum to EDX done on a bulk Bi_2Se_3 single crystal (also plotted in Fig. S3c, red line) shows that the ratio between the Bi and Se peaks is the same for both bulk an the nanocrystal (for V_{acl} = 5 kV). It also clearly shows the disappearance of contributions from the Mica substrate (O, Al, Si peaks) going from the thin crystal to the bulk.

[1] J. G. Analytis, J.-H. Chu, Y. Chen, F. Corredor, R. D. McDonald, Z. X. Shen, I. R. Fisher *Phys. Rev. B*, **81**, 205407 (2010)

[2] L. J. Sandilands, J. X. Shen, G. M. C. F. Zhao, S. Ono, Y. Ando, K. S. Burch, *Phys. Rev. B*, **82**, 064503 (2010)

[3] K. M. F. Shahil, M. Z. Hossain, D. Teweldebrhan, A. A. Balandin, *Appl. Phys. Lett.*,**96**, 153103 (2010)

[4]D. Teweldebrhan, V. Goyal, A. A. Balandin *Nano Lett.*, **10**, 1209 (2010)

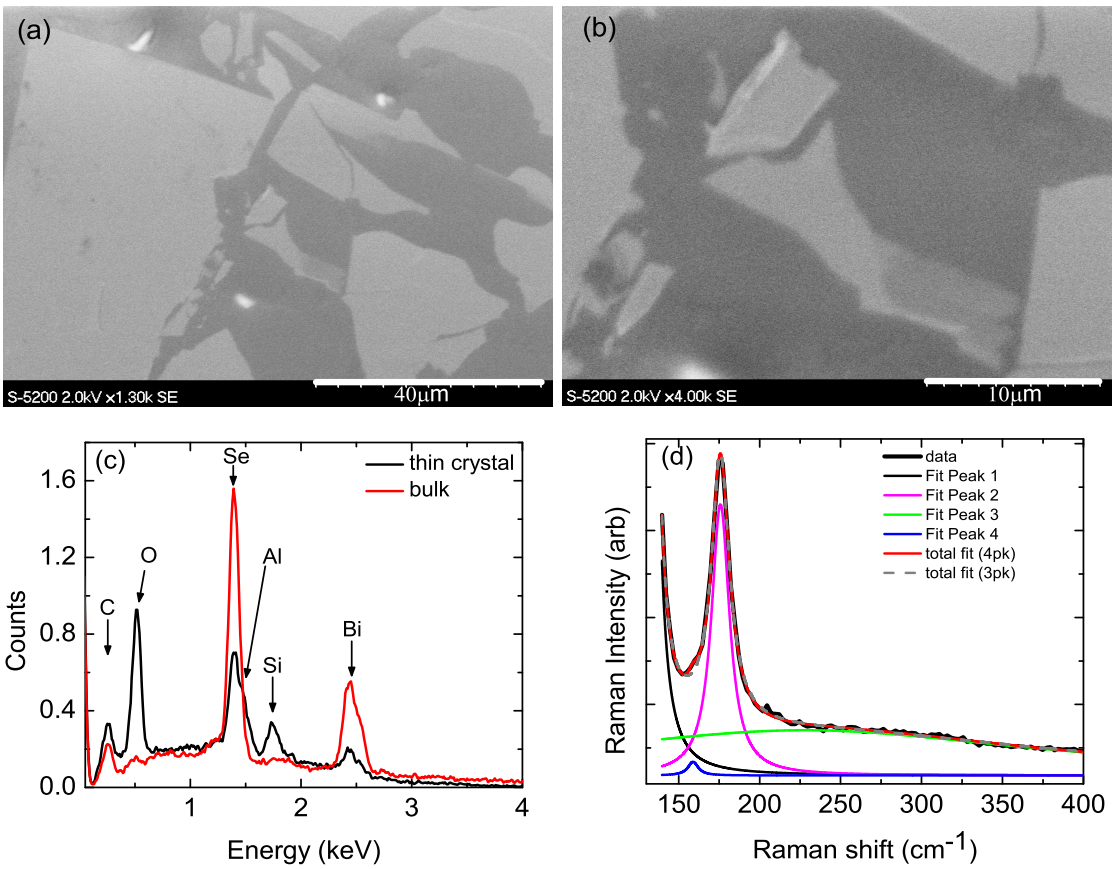

FIG. S3. (a) Scanning electron microscope image of Bi_2Se_3 nanocrystals, the scale bar is 40 μm. (b) Scanning electron microscope image of 4 QL crystal, the scale bar is 10 μm. (c) Energy dispersive X-ray spectrum of the bulk single crystal (red line) and the nanocrystal (black line) shown in (b). (d). Raman spectrum of the 4 QL region also showing a fit consisting of 3 (gray dashed line) and 4 lorentzians (red solid line).